REACTOR MODEL FOR STARCH LIQUEFACTION AND SACCHARIFICATION

Prepared by
Name: Spyros Ploussiou (sp872) College: Wolfson College Date: 18/05/2020

1 Introduction

The main objective of this design was to create a reactor system to liquefy and saccharify gelatinised wheat starch into a glucose solution for further processing. The required production rate of glucose was 71 900 kg h^{-1}. This was the mass flowrate necessary to meet the annual production rate of biobutanol of 100 000 t y^{-1}. Kinetic data from literature was critically assessed prior to being employed for the development of a viable reactor model that will eventually deliver the required 71 900 kg h^{-1} of glucose.

A sensitivity analysis on the effect the most critical parameters of the reactor model have on its output was also conducted and this allowed determination of the optimal saccharification reactor volume and temperature.

Furthermore, specifications for pieces of process equipment necessary to supplement the reactor system, were also estimated. These include 2 shell and tube heat exchangers of different duties and a centrifugal pump.

In the remainder of this report, the assumptions and relevant information that lead to the design of the reactor system are explained, the design aspects of the system are described and the effects that changing reactor temperature and volume have on the output of the system are quantitatively assessed. In addition, data sheets are provided for all the relevant pieces of process equipment.

2 Detailed design model of reactor system

2.1 Reaction kinetics used in modelling the conversion of wheat starch to glucose

The kinetic framework used in describing the conversion of gelatinised wheat starch to glucose was developed by Akerberg et al. **[1]**. Details on it can be found in appendix 8.1 and 8.2.

This model was employed in the design because it was developed with the aim of identifying the optimal reaction conditions for the saccharification process. The influence of variables such as solution pH, α-amylase and glucoamylase concentrations as well as the concentration of starch after liquefaction, were considered in the model**.**

The only temperature-dependent kinetic parameters were assumed to be those listed in table 14 of appendix 8.1. In addition, the parameters listed in table 13 of appendix 8.1, are the ones that were specifically used in the simulation presented by Akerberg et al., and the ones employed in the development of the reactor system.

In the design of the reactor system, a batch time for liquefaction was assumed using additional information gathered from literature. This was compared to the laboratory batch time of 15 minutes reported by Akerberg et al., which occurred at a reaction-medium temperature of 90 ^{o}C. For the purposes of designing the industrial-scale liquefaction reactor, a liquefaction reactor batch time of 1 hour, excluding down-time, was assumed **[2]**.

Equations 1-8 which can be found in appendix 8.2, were solved numerically to determine the variation in concentration of sugars G_n. The subscript n refers to degree of polymerisation and glucose is equivalent to G_1. The initial conditions used for G_n are listed in table 1. These were the initial conditions used in the simulation by Akerberg et al. for the laboratory experiment carried out at a pH of 5, temperature of 55 ^{o}C, S_o of 18.8 g dm^{-3}and E_{AMG} and E_a of 0.885 and 0.109 mm^3 (g starch)$^{-1}$ respectively. This was the recommended set of most optimal laboratory reaction conditions.

Table 1: Initial conditions of G_n (g dm^{-3}) in simulation conducted by Akerberg et al. at most optimal conditions determined by laboratory experiments

G_1	G_2	G_3	G_4	G_5	G_6	G_7	G_{Large}
2.3	1.9	0.092	0.36	0.14	0.62	0.24	13

The evolution of each G_n with time, using the initial conditions presented in table 1, is depicted in figures 1 and 2.

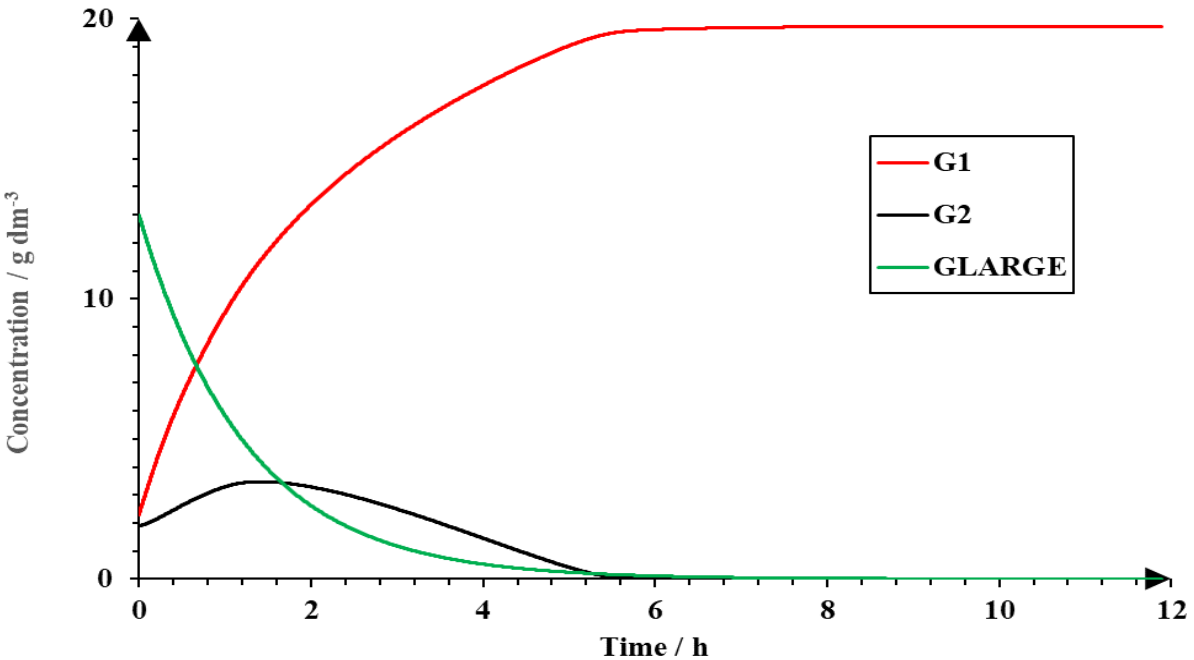

Figure 1: Evolution of G_1, G_2 and G_{Large} at S_o of 18.8 g dm^{-3} and most optimal conditions for saccharification determined at the laboratory scale

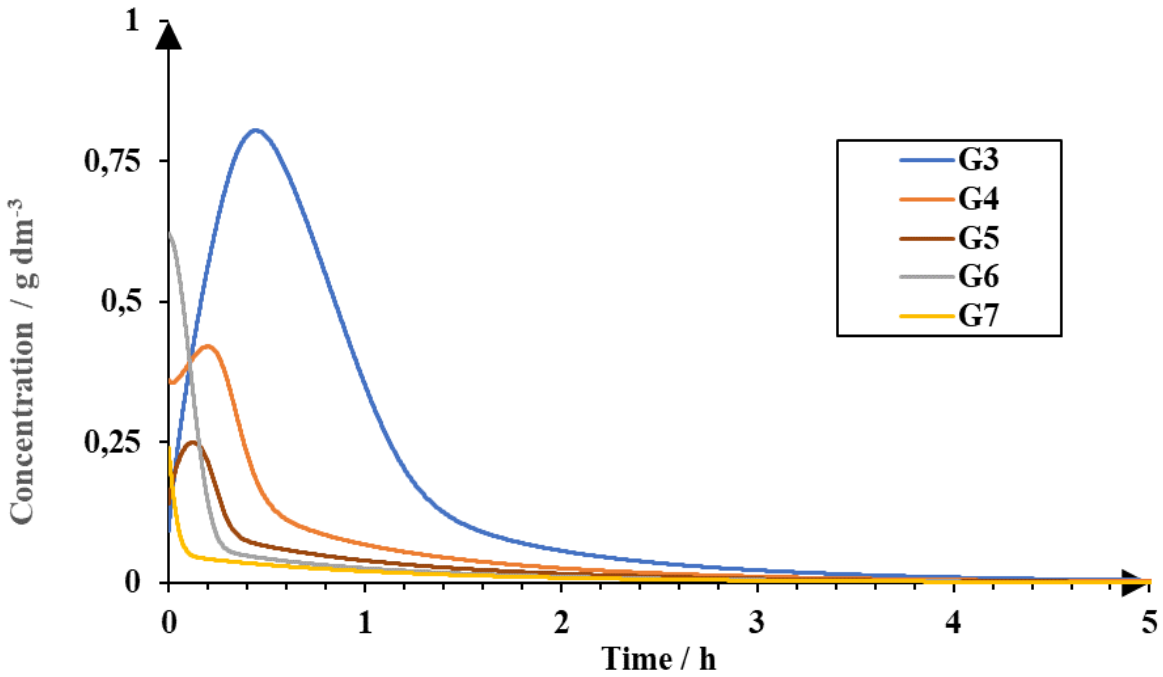

Figure 2: Evolution of G_n for n = 3-7 at *S_o of 18.8 g dm^{-3} and most optimal conditions for saccharification determined at the laboratory scale*

Figures 1 and 2 suggest that complete conversion of liquefied wheat starch occurs at approximately 6 hours. The concentrations of other species become negligible by then. When solving equations 1-8, sharp changes in concentration gradients were noticed at large time steps. The time interval used in the numerical approach was reduced to 0.36 seconds to avoid missing potential salient points in the concentration profiles of each G_n. Furthermore, the total sugar concentration was plotted against time as shown in figure 3. This was performed to verify conservation of mass.

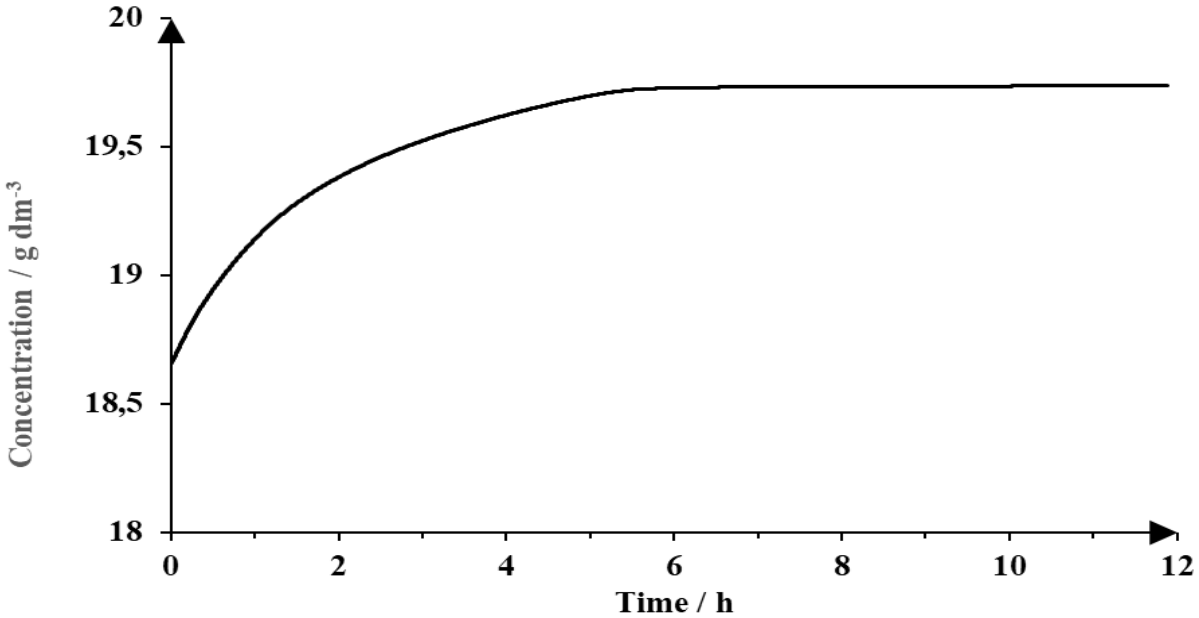

Figure 3: Evolution of total sugar concentration in solution at *S_o of 18.8 g dm^{-3} and most optimal conditions for saccharification determined at the laboratory scale*

According to figure 3, there is a small discrepancy in the total mass of the system modelled, of approximately 5.1 %. This is not a very significant uncertainty, but it is likely that it arises because of the assumptions employed in the model by Akerberg et al. It is likely to have an influence on the validity of the batch time chosen for the industrial-scale process that is to produce 71 900 kg h^{-1} of glucose.

2.2 Assumptions employed in developing the reactor system that meets the glucose production specification

The concentration of glucose required for further processing was specified at 60 g dm^{-3} by the Area 4, ABE fermentation, engineer.

If the initial concentration of liquefied starch S_o required in the saccharification reactor of the reactor system is assumed to be 18.8 g dm^{-3} at inlet conditions, then the need to concentrate the resultant glucose solution to 60 g dm^{-3} arises. To avoid additional operating and capital costs that come with the equipment that concentrates the glucose solution, a reactor system was designed for saccharification inlet S_o of 60 g dm^{-3}. The E_a, E_{AMG}, pH and saccharification reactor temperature were assumed to be the same as the optimal values determined by Akerberg et al. at the laboratory-scale.

The set of equations 1-8 in appendix 8.2 were also solved at these conditions and the main assumption employed was that the initial conditions of G_n listed in table 1 changed by a scale factor of 60/18.8. This scale factor of 3.19 was assumed to be small enough not to generate excessive uncertainty **[3]**. The new initial conditions of G_n are listed in table 2. In addition, figure 4 depicts the evolution of each G_n using the relevant initial conditions.

Table 2: Initial conditions of G_n (g dm^{-3}) used based on re-scaling assumption

G_1	G_2	G_3	G_4	G_5	G_6	G_7	G_{Large}
7.3	6.1	0.29	1.1	0.45	2.0	0.77	41

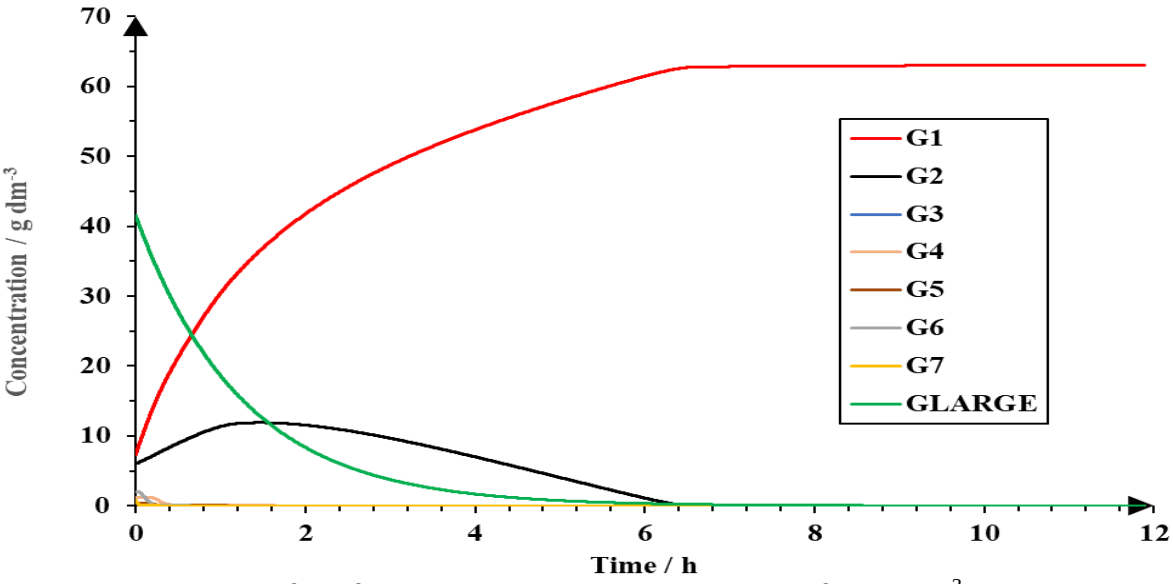

Figure 4: Evolution of G_n for n = 1-7 including G_{Large} at S_o of 60 g dm^{-3} and most optimal conditions for saccharification determined at the laboratory scale

Conservation of total sugar mass was also tested at S_o = 60 g dm^{-3} and a discrepancy of 4.9 % was observed. Given that the scale factor by which the initial conditions changed was not substantially large, it was deemed reasonable to design a reactor system with the aim of producing approximately 60 g dm^{-3} of glucose solution for S_o = 60 g dm^{-3}. According to figure 4, the laboratory batch time at these parameter values is approximately 6.3 hours.

When designing the batch reactor system including both liquefaction and saccharification, a total batch time of 10 h was assumed, after careful consideration of mass transport limitations and down-time due to cleaning and maintenance. This was decided even though liquefaction and saccharification take approximately 1 and 6.3 h, respectively.

The necessary mass flowrate of gelatinised wheat starch going into the reactor system was estimated by assuming 100 % conversion of gelatinised wheat starch to glucose, based on the results acquired from the model developed by Akerberg et al. In addition, the fact that some water is consumed during liquefaction and saccharification, was also accounted for.

For an overall batch time of 10 h, the glucose capacity of the system must be 719 000 kg. As a result, the required mass of starch must also be 719 000 kg. The gelatinised starch stream coming from Area 2 (gelatinisation of wheat starch) also contains some glucose and approximately 152 837 kg h^{-1} of water. Based on these, the starch capacity of the system designed was assumed to be approximately 71 500 kg/h or 715 000 kg after considering the 10 h of total batch time.

2.3 Detailed design of liquefaction reactor system

The overall reactor system designed to meet the necessary glucose specification involves 10 batch lines. Onto each line there is a liquefaction reactor followed by a saccharification reactor. The overall reactor volume of the system was initially estimated at 38 244 m^3 for S_o = 18.8 g dm^{-3}. This was performed by dividing the glucose capacity of the system of 719 000 kg by 18.8 g dm^{-3}.

Splitting the entire system into 10 batches does not alter the S_o along each batch line. As a result, each batch line will have a reactor volume of approximately 3 820 m^3. Using the assumption that liquefaction and saccharification take place in approximately 2 and 8 h respectively (total of 10 h), including down-time, the volume of the liquefaction reactor along each batch line was estimated at 764 m^3. This was performed by using the ratio between liquefaction batch time and total batch time. Similarly, the saccharification reactor volume along each batch line was estimated at 3 056 m^3.

Increasing S_o to 60 g dm^{-3} reduced the overall reactor volume to 11 980 m^3. The new reactor volumes along each batch line were estimated in a similar manner at 239.7 m^3 and 958.7 m^3 for liquefaction and saccharification, respectively.

For the design of the liquefaction reactor, a viscosity for the gelatinised wheat starch stream of approximately 2 Pa s was assumed. In addition, a conservative value of density of 985 kg m^{-3} was employed **[4]**. These assumptions allowed designing for the most extreme fluid conditions in the reactor system.

Each of the 10 liquefaction reactors of volume 239.7 m^3 was designed to achieve the highest possible degree of mixing and agitation. A stirred tank vessel configuration was specified for

this reactor. The membrane and loop reactors were eliminated because of their added complexity and more stringent operating condition requirements **[5]**.

The reactor was designed to include the internal equipment listed in table 3.

Table 3: Internal equipment of liquefaction reactor

Internals	Number of units
Baffles	4
Six-blade pitched (45^{o}) turbine	2
Eductor agitation nozzles	2
Stainless steel screen (mesh)	1
Spray bulbs for tank washing	2

The position and size of the internal equipment were estimated by assuming an aspect ratio of 1 for the cylindrical vessel. As a result, its diameter was estimated at 6.732 m. For an aspect ratio of 1, the height of liquid in the vessel was assumed to be equal to the height of the vessel. At this aspect ratio there are well established charts for mixing in bioreactors, that relate the power number to the Reynolds number of the impeller within the vessel.

A 6-blade impeller with an angle of pitch of 45^{o} was chosen instead of a Rushton impeller. This kind of impeller is better suited for the mixing of gelatinised starch since it can handle more viscous fluids.

For a 6-blade pitched turbine, turbulent flow is established at Reynolds numbers of at least 10^3. Using the aspect ratio of 1 and specifying the Reynolds number at 5000, allowed calculation of parameters such as impeller diameter and baffle width.

Figure 5 depicts a drawing of the liquefaction reactor unit including dimensions which are not drawn to scale.

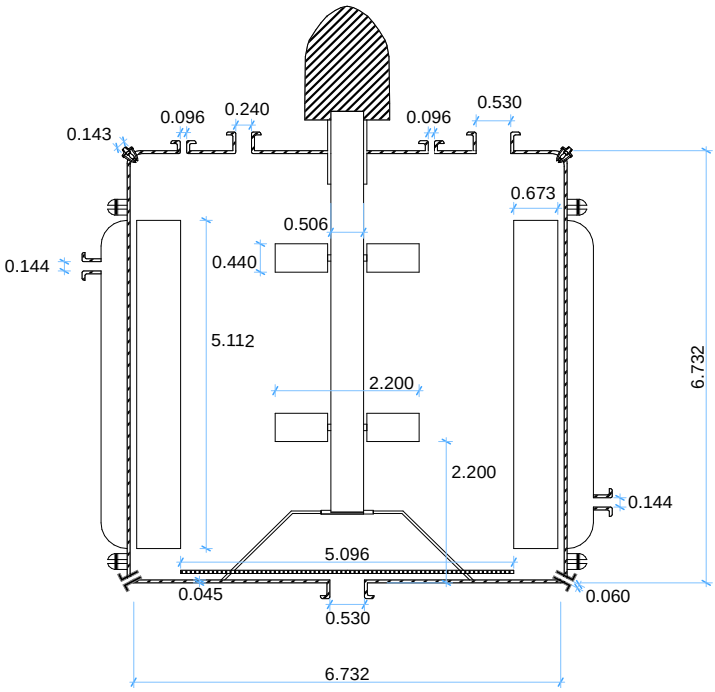

Figure 5: 2-D section of the liquefaction reactor. Dimensions are in metres

Dimensional analysis using appropriate ratios of variables such as tank diameter and impeller diameter were employed in estimating values for the parameters shown in figure 5 and listed in table 4.

Table 4: Dimensions of liquefaction reactor key internal parameters

Parameter	Dimension / m
Impeller diameter	2.20
Impeller blade width	0.44
Clearance of Baffles from reactor wall	0.13
Baffle width	0.67
Distance of impeller from the bottom of the reactor	2.20
Distance between impellers	2.20

The power requirement for mixing was estimated at the fixed Reynolds number of 5000. For an aspect ratio of 1 the power number of the 6-blade pitched (45^o) impeller is approximately 1.3. The rotational speed of the impeller was estimated at 123 rpm using the definition of the impeller Reynolds number. It was assumed that for a 2-impeller system the necessary power number is twice that of a single impeller system. In addition, the power requirement of the agitation system of each liquefaction reactor was estimated at 1.21 MW using the definition of the power number for an impeller diameter of 2.20 m. **[6]**.

Two impellers were employed in the design of the liquefaction reactor to ensure adequate mixing for a reactor volume of 239.7 m^3. The diameter of the shaft connecting the impellers to the main electric motor unit was estimated at 0.506 m using the relationship between power and shaft diameter for main power transmitting shafts with keyway. This was performed by assuming an electric motor efficiency of 0.1 since, these units typically have low efficiencies **[7]**.

Figure 6 shows a model of the 2 six-blade pitched (45^o) impellers mounted on the 0.506 m diameter shaft.

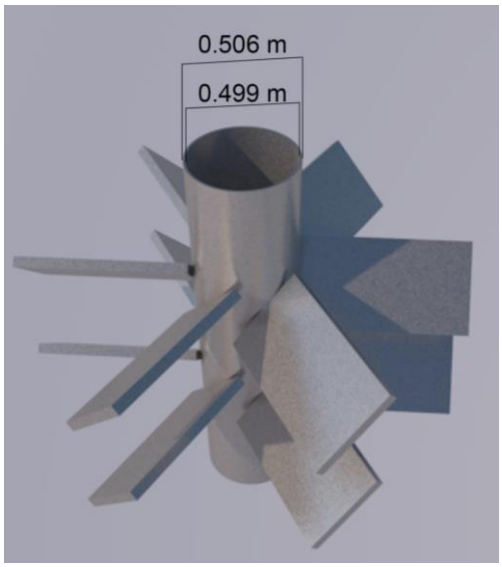

Figure 6: 3-D model of liquefaction reactor main agitation equipment

All associated internal equipment including the vessel itself were assumed to be made of grade 304 stainless steel. This material has better corrosion and heat resistance than other materials such as carbon steel. In addition, the material of the internal equipment must be compatible with the material make-up of the reactor itself.

The density of grade 304 stainless steel of 8 060 kg m^{-3} was used to calculate the mass of each liquefaction reactor at 50 836 kg. The actual mass including the internal equipment is approximately double this value.

A data sheet for the liquefaction reactor can be found in section 5. The vessel was designed at a pressure of 5 bar even though it will be operated at approximately 1.8 bar. The thicknesses of the liquefaction reactor wall and cylindrical shaft supporting the impellers were estimated using the relationship for hoop stress in cylindrical pressure vessels and a stress value of 380 MPa which is 80 % the yield stress of grade 304 stainless steel **[8]**. These are listed in table 5.

Table 5: Estimated thickness of the liquefaction reactor and shaft connecting turbines to main motor driving unit. The values recorded are 10 times the minimum ones estimated

Parameter	Thickness / mm
Liquefaction reactor wall	44.3
Cylindrical shaft	3.33

The reactor will normally operate between 55 and 90 ^{o}C. This is because the gelatinised wheat starch stream entering the reactor at approximately 55 ^{o}C will have to be warmed to 90 ^{o}C which is the optimal temperature for liquefaction according to Akerberg et al. A heating jacket is sufficient for this reactor volume.

The required heating duty of each liquefaction reactor was estimated at 5.4 MW using the assumption that the heat capacity of the reactor content is that of water between 55-90 ^{o}C, of 4.2 kJ kg^{-1} K^{-1}. The duty will be met by low pressure steam at 1.77 bar and 133 ^{o}C.

Furthermore, this reactor will consist of no immobilised enzymes since α-amylase will already be present in solution. In addition, nutrients and water will be added to the reactor.

2.3 Detailed design of saccharification reactor system

A stirred tank vessel configuration was also specified for the saccharification reactor. A data sheet for this reactor can also be found in section 5.

The same method as for the liquefaction reactor was employed in designing this reactor. The main differences include the possibility of even more extensive heat and mass transfer limitations within the saccharification reactor because its volume of 958.7 m^3 is approximately 4 times larger. Glucoamylase and α-amylase will be added to this reactor as well as sulfuric acid, to reduce the pH to the desired value of 5. The enzymes will be immobilised in calcium alginate beads **[9]** and re-used at the end of each batch.

Figure 7 depicts a drawing of the saccharification reactor including dimensions which are not drawn to scale. In addition, table 6 lists the internal equipment of the saccharification reactor.

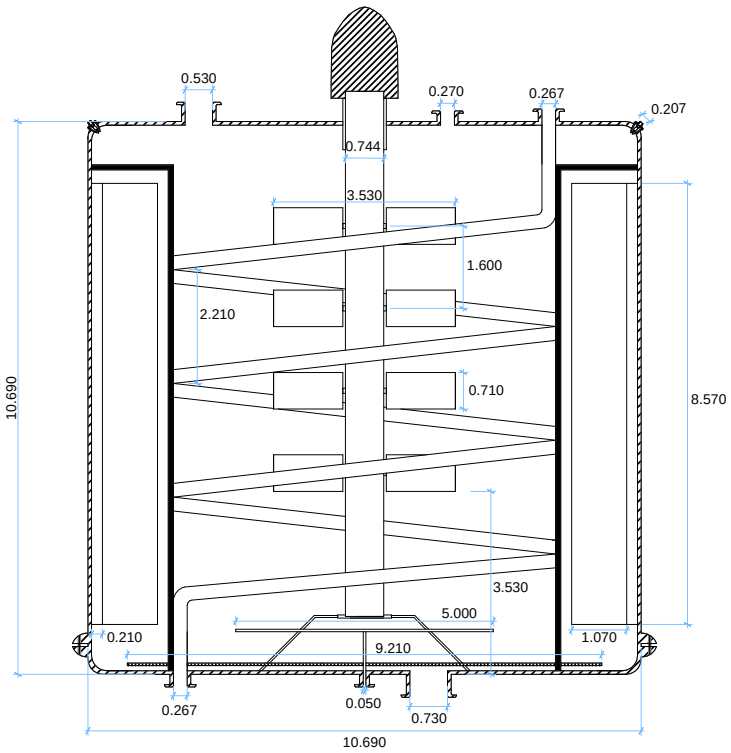

Figure 7: 2-D section of saccharification reactor. Dimensions are in metres

Table 6: Internal equipment of saccharification reactor

Internals	Number of units
Baffles	4
Six-blade pitched (45^{o}) turbine	4
Stainless steel screen (mesh)	1
Spray bulbs for tank washing	2

The saccharification reactor will normally operate at approximately 1.6 bar between 55-90 ^{o}C. The cooling will be performed by internal supported helical coils carrying cooling water at 20 ^{o}C and 5 bar. This will ensure better heat transfer as opposed to an external cooling jacket, because of the size of the reactor.

A nitrogen sparger will also be positioned at the bottom of the reactor to ensure more adequate mixing in case the 4 turbines providing agitation are not sufficient. As a result, additional pressure relief devices such as a burst drum are included in its design. The same principles and physical properties of fluids used in the design of the liquefaction reactor were also employed when sizing each of the 10 saccharification reactors. Table 7 lists the estimated dimensions of the saccharification reactor and its internals.

Table 7: Associated saccharification reactor parameter dimensions

Parameter	Dimension / m
Reactor height	10.69
Reactor diameter	10.69
Impeller diameter	3.53

Impeller blade width	0.71
Clearance of baffles from reactor wall	0.21
Baffle width	1.07
Distance of impeller from the bottom of the reactor	3.53
Distance between impellers	1.60
Diameter of coil carrying cooling water	0.27
Pitch of helix formed by coils carrying cooling water	2.21

The rotational speed and power requirement of the agitation system of each saccharification reactor were estimated at 49 rpm and 1.52 MW, respectively. It was assumed that for a 4-impeller system the necessary power number is 4 times that of a single impeller. The diameter of the shaft connecting the impellers to the main electric motor unit was estimated at 0.744 m, using the same assumptions employed in the design of the liquefaction reactor.

Figure 8 depicts a model of the 4 six-blade pitched (45^{o}) impellers mounted on the 0.744 m diameter shaft.

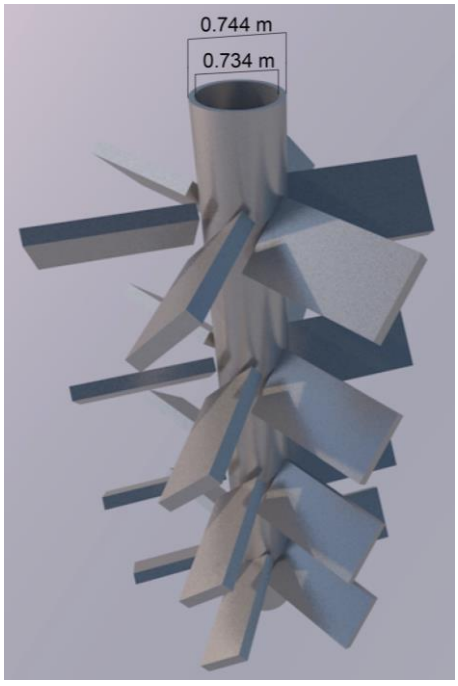

Figure 8: 3-D model of saccharification reactor main agitation equipment

The required cooling duty of each saccharification reactor was estimated at 4.8 MW using the assumption that the heat capacity of the reactor content is that of water between 55-90 ^{o}C, of 4.2 kJ kg^{-1} K^{-1}. This was a reasonable assumption since the contents of the reactor will mainly be water.

The saccharification reactor was also designed to operate at a pressure of 5 bar. The thicknesses of the reactor wall and the cylindrical shaft operating the impellers were also estimated using the relationship for hoop stress in cylindrical pressure vessels and a stress value of 80 % the

yield stress of grade 304 stainless steel. The relevant thicknesses are listed in table 8. The mass of each saccharification reactor was calculated at 203 420 kg using the density of grade 304 stainless steel. The actual mass including the internal equipment is approximately 2 times this value.

Table 8: Estimated thickness of the saccharification reactor and shaft connecting turbines to main motor driving unit. The values recorded are 10 times the minimum ones estimated

Parameter	Thickness / mm
Saccharification reactor wall	70.3
Cylindrical shaft	4.89

3 Sensitivity analysis

3.1 Analysis on effect that saccharification reactor temperature has on the glucose output of the system

The liquefaction reactor on each batch line will operate at 90 ^{o}C. This is the optimal temperature for liquefaction according to Akerberg et al. and T. Komaki et al. **[10]**. The saccharification reactor temperature will have the dominant effect on the output of the overall reactor system since it involves the conversion of the partially hydrolysed starch to glucose. For the purposes of the sensitivity analysis it was assumed that E_a and E_{AMG} are 0.885 and 0.109 mm^3 $(g\ starch)^{-1}$ respectively.

The only temperature dependent parameters in the model developed by Akerberg et al. are those listed in table 14 of appendix 8.1. Figure 9 depicts the evolution of each G_n in the scenario that the temperature of the saccharification reactor drops to 30 ^{o}C.

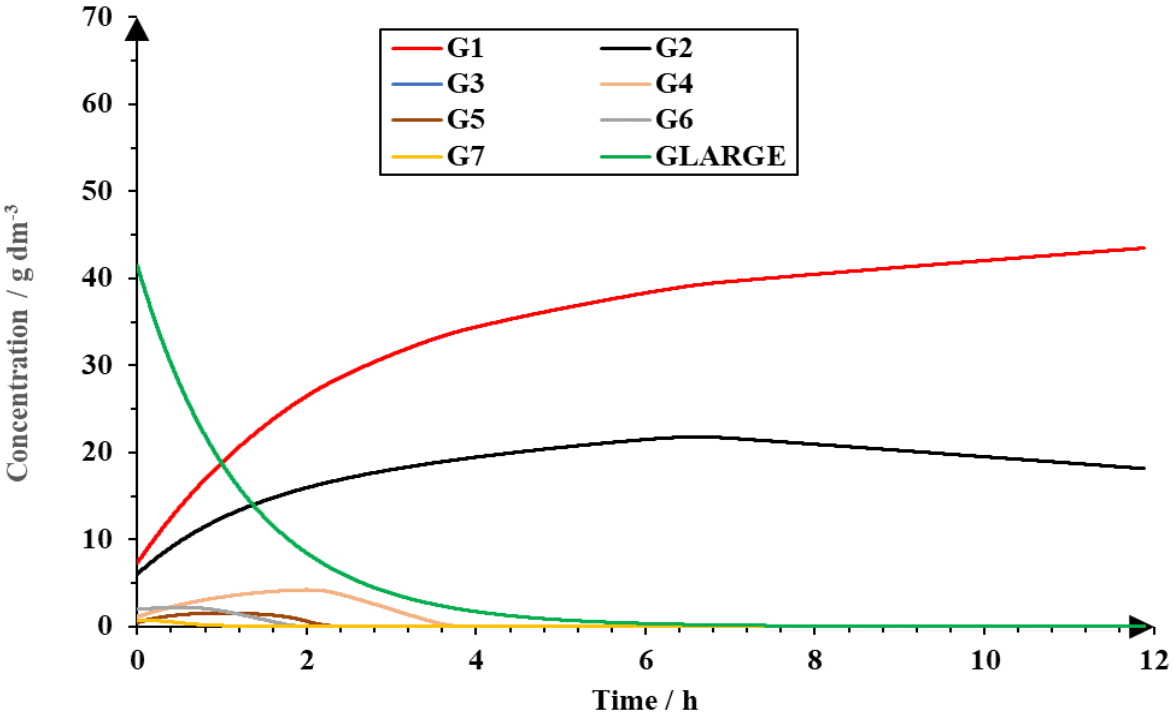

Figure 9: Evolution of G_n for n = 1-7 including G_{Large} at S_o of 60 g dm^{-3} at 30 ^{o}C, pH of 5

According to figure 9, and assuming a saccharification batch time of 8 hours (as in the reactor model), the glucose productivity is approximately 40 g dm^{-3} at 30 ^{o}C. In addition, maltose is also present at approximately 18 g dm^{-3}.

For temperatures between 30 and 55 ^{o}C, an Arrhenius relationship of the form $a_o exp^{-E/RT}$ was assumed for the kinetic constants listed in table 14 of appendix 8.1. In the Arrhenius expression a_o, E and R are the Arrhenius constant, Arrhenius activation energy and universal gas constant, respectively. This assumption was employed because the relevant parameters appear in rate equations for which no other temperature dependence was specified, according to Akerberg et al. Tables 9 and 10 list the Arrhenius parameter fittings for the relevant kinetic parameters.

Table 9: Arrhenius parameters for k_{esm}

Akerberg model parameters	**Arrhenius parameter fittings**	
	Arrhenius constant / 10^{22} g dm^{-3}	**Arrhenius activation energy / 10^3 J mol^{-1}**
k_{esm}	8.44	53.38

Table 10: Arrhenius parameters for $k_{1,m}$ to $k_{7,m}$

Akerberg model parameters	**Arrhenius parameter fittings**	
	Arrhenius constant / h^{-1}	**Arrhenius activation energy / 10^3 J mol^{-1}**
$k_{1,m}$	0.20	-3.52
$k_{2,m}$	4.69×10^{-10}	-53.49
$k_{3,m}$	9.08	8.81
$k_{4,m}$	1.79	4.15
$k_{5,m}$	0.47	0.41
$k_{6,m}$	33.29×10^{5}	43.84
$k_{7,m}$	364.43	16.47

In addition, table 11 lists the concentrations of G_1, G_2 and G_{LARGE} at different temperatures within the range of 30-55 ^{o}C after 8 hours of batch time. The other species had negligible concentrations at this point.

Table 11: Concentration of G_1, G_2 and G_{LARGE} at different temperatures after 8 hours of batch time

Temperature / ^{o}C	**G_1 / g dm^{-3}**	**G_2 / g dm^{-3}**	**G_{LARGE} / g dm^{-3}**
30	40.46	20.94	0.07
31	41.30	20.15	0.08
32	42.15	19.36	0.08
33	43.01	18.55	0.09
34	43.87	17.74	0.09
35	44.75	16.92	0.09
36	45.65	16.08	0.10
37	46.56	15.23	0.10
38	47.48	14.36	0.10

39	48.43	13.47	0.10
40	49.40	12.56	0.10
41	50.40	11.63	0.10
42	51.42	10.68	0.10
43	52.48	9.69	0.10
44	53.56	8.68	0.10
45	54.68	7.63	0.10
46	55.84	6.55	0.10
47	57.03	5.44	0.10
48	58.23	4.30	0..10
49	59.52	3.11	0.09
50	60.80	1.91	0.09
51	62.06	0.73	0.08
52	62.84	0.01	0.08
53	62.87	0.00	0.08
54	62.89	0.00	0.07
55	62.91	0.00	0.07

When interpreting the results shown in table 11, the discrepancy in conservation of mass of the system was accounted for. Given a degree of uncertainty equivalent to the discrepancy in conservation of mass, the optimal saccharification reactor temperature is 55 ^{o}C. At 55 ^{o}C, G_1 = 62.91 g dm^{-3}. The total mass of the system is 60 g dm^{-3}. As a result, the uncertainty is approximately 4.9 %.

The Arrhenius relationship developed, fails out of the 30-55 ^{o}C range, which is sensible given that the kinetic parameter values used were experimentally determined at only 2 different temperatures.

At temperatures less than 30 ^{o}C the glucose productivity is bound to be low due slow kinetics. Moreover, at temperatures greater than 55 ^{o}C, glucose productivity is also expected to decrease relative to that at 55 ^{o}C. This is because the optimal temperature of glucoamylase is approximately 55 ^{o}C. At temperatures close to 55 ^{o}C, glucose productivity will not change substantially. Large temperature swings are necessary for this to happen.

3.2 Analysis on effect that saccharification reactor volume has on the glucose output of the system

The reactor system designed involves 10 batch lines and each has saccharification and liquefaction batch times of approximately 8 and 2 h, respectively. The overall necessary liquefaction reactor volume was specified at 2 397 m^3. The required production rate and concentration of glucose entering Area 4 are 71 900 kg h^{-1} and 60 g dm^{-3}, respectively. These were the constraints used in the relevant sensitivity analysis.

In performing the sensitivity analysis, the glucose concentration resulting from each saccharification reactor was estimated by multiplying the required glucose production rate by 10 h (total assumed batch time) and dividing by the total reactor volume (both liquefaction and saccharification), part of which was specified at 2 397 m^3. Table 12 lists the results of this analysis.

Table 12: Effect that saccharification reactor volume on each batch line has on glucose output

Saccharification reactor volume / m^3	**G_1 / g dm^{-3}**
550	91.05
600	85.63
650	80.82
700	76.52
750	72.65
800	69.16
850	65.98
900	63.09
950	60.44
1000	58.00
1050	55.75
1100	53.67

It is clear from the results shown in table 12 that, to meet the 60 g dm^{-3} concentration requirement and 71 900 kg h^{-1} glucose production rate, each batch line must have a saccharification reactor volume between the values of 950-1000 m^3. The exact value was estimated at 958.7 m^3.

4 Conclusions

The necessary saccharification reactor volume and temperature were identified at 958.7 m^3 and 55 ^oC, respectively. These conditions were determined by specifying several other variables such as overall liquefaction reactor volume.

Other process areas of the biobutanol production plant that are affected by the stated choices of conditions include Area 2 and Area 4. Area 2 will not be significantly affected by these conditions. On the contrary, Area 4 will be affected. The saccharification reactor product will be pumped at a temperature of 55 ^oC to a pressure greater that 1.5 bar. Cooldown of this stream to 35 ^oC will be required prior to entry into Area 4.

5 Equipment data sheets

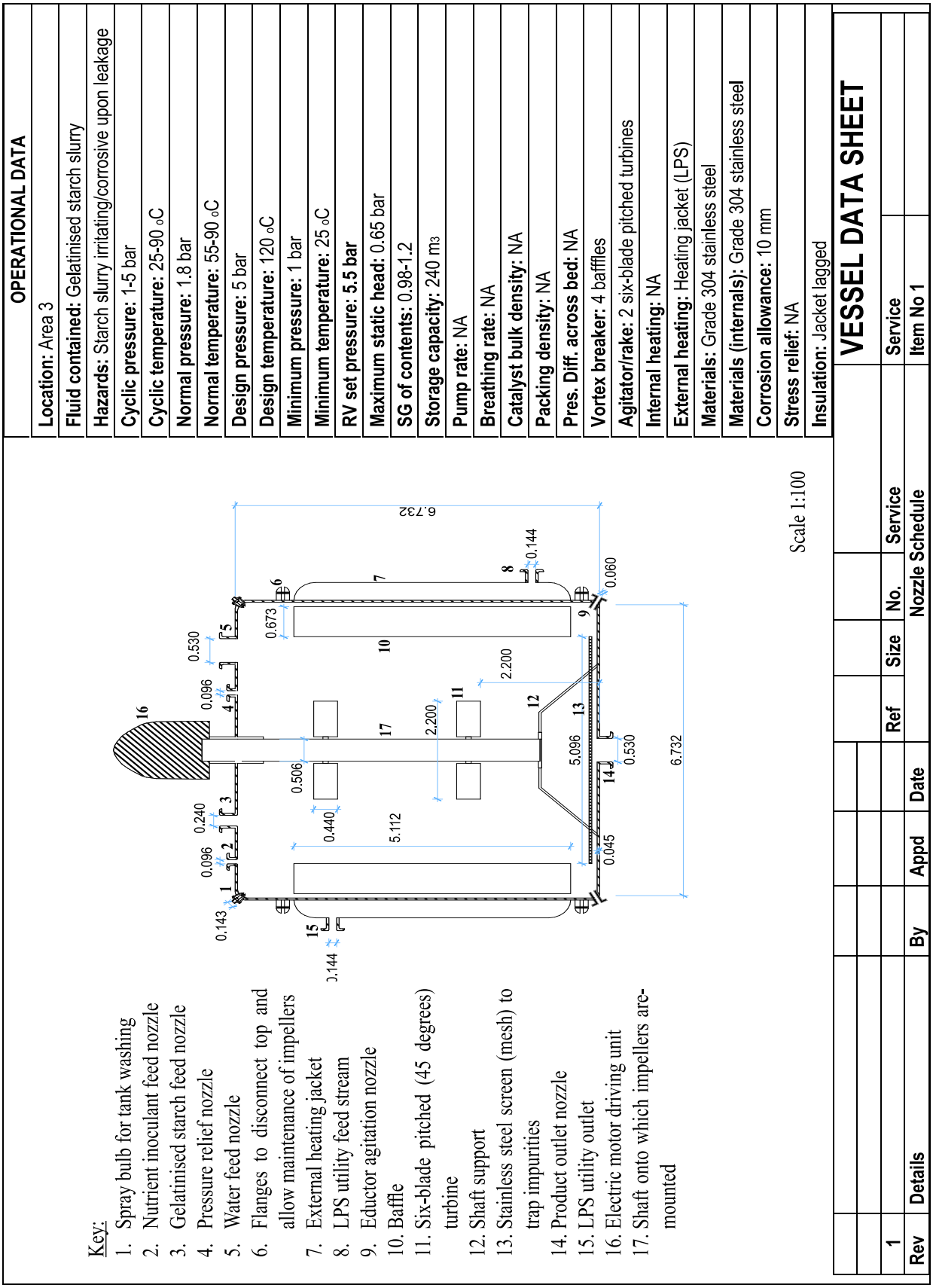

Key:

1. Spray bulb for tank washing
2. Partially hydrolysed gelatinised starch feed nozzle
3. Immobilised enzyme feed nozzle
4. Cooling water outlet nozzle
5. Flanges to disconnect top and allow maintenance of impellers
6. Product outlet nozzle
7. Sparged nitrogen inlet nozzle
8. Stainless steel screen to trap and reuse immobilised enzymes
9. Internal cooling coil support
10. Six-blade pitched (45 degrees) turbine
11. Baffle
12. Cooling water inlet nozzle
13. Shaft onto which impellers are mounted
14.. Shaft support

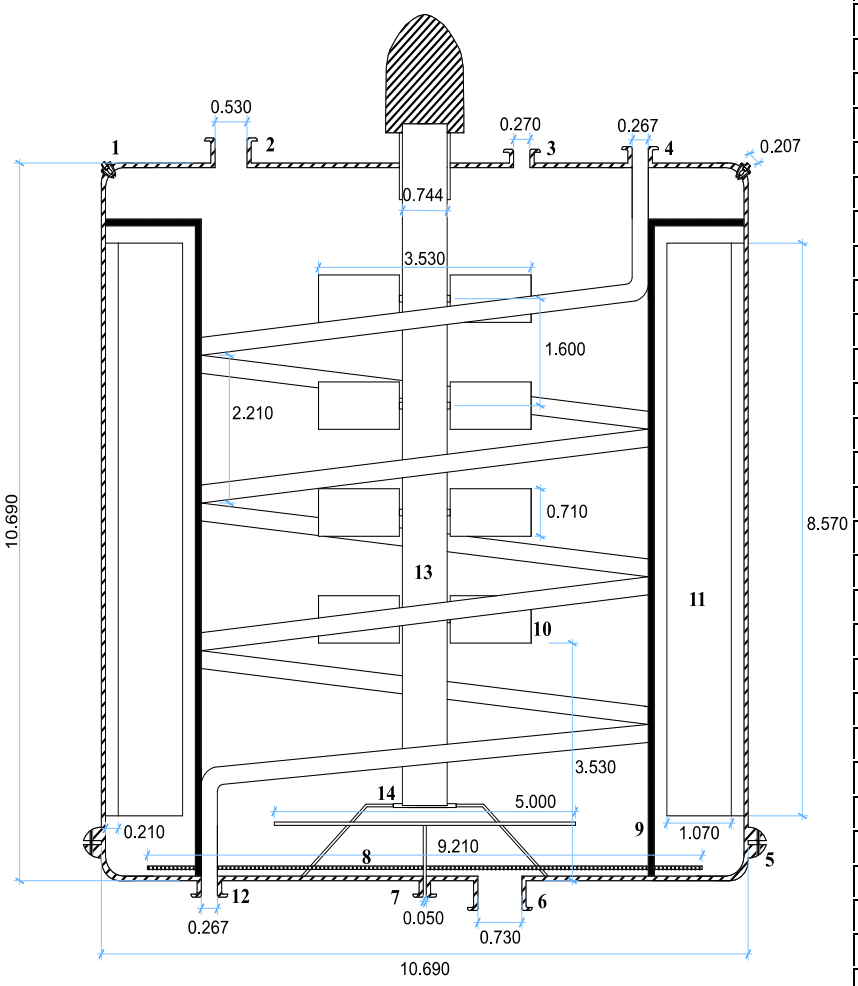

OPERATIONAL DATA
Location: Area 3
Fluid contained: Partially hydrolysed starch slurry
Hazards: Starch slurry irritating/corrosive upon leakage
Cyclic pressure: 1-5 bar
Cyclic temperature: 25-90 $_{o}$C
Normal pressure: 1.6 bar
Normal temperature: 55-90 $_{o}$C
Design pressure: 5 bar
Design temperature: 120 $_{o}$C
Minimum pressure: 1 bar
Minimum temperature: 25 $_{o}$C
RV set pressure: 5.5 bar
Maximum static head: 1.03 bar
SG of contents: 0.98-1.2
Storage capacity: 959 m$_{3}$
Pump rate: NA
Breathing rate: NA
Catalyst bulk density: NA
Packing density: NA
Pres. Diff. across bed: NA
Vortex breaker: 4 bafffles
Agitator/rake: 4 six-blade pitched turbines
Internal heating: Cooling water helical coils
External heating: NA
Materials: Grade 304 stainless steel
Materials (internals): Grade 304 stainless steel
Corrosion allowance: 10 mm
Stress relief: NA
Insulation: Vessel lagged

									VESSEL DATA SHEET	
1					**Ref**	**Size**	**No.**	**Service**	**Service**	
Rev	**Details**	**By**	**Appd**	**Date**	**Nozzle Schedule**				**Item No 2**	

HEAT EXCHANGER DATA SHEET

Client CEB	**Area 3**	**Item no. 3**

Service Towns water heating from 20 °C to 55 °C		
No of units 1	**Type** AES	**Orientation** Horizontal

	Units	**Shell Fluid (Towns water)**		**Tube Fluid (LPS)**	
		In	**Out**	**In**	**Out**
Total fluid flow	**kg s^{-1}**	266.5	266.5	778	778
Liquid	**kg s^{-1}**	266.5	266.5	0	0
Vapour	**kg s^{-1}**	0	0	778	778
Non-condensable	**kg s^{-1}**	0	0	0	0
Steam	**kg s^{-1}**	0	0	778	778
Water	**kg s^{-1}**	266.5	266.5	0	0
Temperature	**°C**	20.0	55.0	131.0	102.5
Mol. Wt of vapour + NC		0	0	1.0	1.0
Liquid density	**kg m^{-3}**	998	985	0	0
Liquid viscosity	**Pa s**	0.0010	0.0005	0	0
Vapour + NC viscosity	**Pa s**	NA	NA	0.000013	0.000012
Liquid sp. heat	**kJ kg^{-1} K^{-1}**	4.18	4.21	NA	NA
Vapour + NC sp. heat	**kJ kg^{-1} K^{-1}**	NA	NA	2.16	2.10
Liquid thermal conductivity	**W m^{-1} K^{-1}**	0.603	0.649	NA	NA
Vap. + NC thermal conduct.	**W m^{-1} K^{-1}**	NA	NA	0.0274	0.0245
Latent heat	**kJ kg^{-1}**	2453.5	2282.5	2211	2257
Surface tension	**N m^{-1}**	0.0723	0.0669	NA	NA
Dew pt/bubble pt	**°C**	151.8	145.0	115.0	100.0
Freeze pt/pour pt	**°C**	0	0	0	0
Inlet pressure	**bar**	5		1.77	
Allowable press. drop	**bar**	0.70		0.77	
Fouling resistance	**m^2 K W^{-1}**	0.00025		0.00009	
Heat exchanged	**MW**	39.36			
Min./max. operating temp	**°C**	15	60	95	135
Max. operating pressure	**bar**	6		3	
Min. design pressure	**bar**	5		2	
Relief valve set pressure	**bar**	6		3	
Design pressure	**bar**	7		4	
Cyclic service		☒		☒	
Materials		Carbon steel		Carbon steel	
Corrosion allowance	**mm**	1.0		1.0	
Line size	**mm**	587	587	800	800
Heat treatment		☒		☒	
Hazards		Moderately pressurised		Hot upon physical contact	
Insulation		NA		NA	
Cleaning		Once every 3 months		Once every 3 months	
Over design multiplier		1.20		2.21	

Remarks				
Rev no 1				
Eng/date				
Checked/date				
Approved/date				

Centrifugal Pump Data Sheet

Client CEB	**Area** 3	**Item no.** 4

Service		
No of units 1	**Type Axial-flow**	**Orientation** Horizontal

	Units	**Shell Fluid (Ethylene glycol)** **Tube Fluid (Cooling water)**
Fluid		
Density	**kg/m^3**	988
Viscosity	**Pa s**	0.54
Temperature	**Deg C**	55.0
Vapour pressure	**Pa**	12000
Solids (type)		NA
Solids %		NA
Flow rate	**m^3/s**	0.336
Suction head	**m**	3.83
Static head	**m**	5.00
Dynamic head	**m**	0.00
Net pump head	**m**	8.83
Est. Efficiency		0.75
Est. Power	**kW**	10.37
NPSH	**m**	7.56
Hazards		Mildly corrosive liquid upon leakage. Moderately high temperature
Materials		Carbon steel
Seal		Hydrodynamic mechanical seal
Seal liquid		Unbalanced mechanical seal
Driver		Electric motor (AC supply)
Drive speed	**rpm**	1675

Remarks				
Rev no 1				
Eng/date				
Checked/date				
Approved/date				

HEAT EXCHANGER DATA SHEET

Client CEB	**Area** 3	**Item no.** 5

Service Glucose solution cooldown from 55 °C to 35 °C		
No of units -	**Type** AES	**Orientation** Horizontal

	Units	**Shell Fluid (Glucose solution)**		**Tube Fluid (Cooling water)**	
		In	**Out**	**In**	**Out**
Total fluid flow	**kg s^{-1}**	332.7	332.7	277.8	277.8
Liquid	**kg s^{-1}**	332.7	332.7	277.8	277.8
Vapour	**kg s^{-1}**	0	0	0	0
Non-condensable	**kg s^{-1}**	0	0	0	0
Steam	**kg s^{-1}**	0	0	0	0
Water	**kg s^{-1}**	310.0	310.0	277.8	277.8
Temperature	**°C**	55	35	18	42
Mol. Wt of vapour + NC		NA	NA	NA	NA
Liquid density	**kg m^{-3}**	1020.0	1022.0	999.0	992.0
Liquid viscosity	**Pa s**	0.00050	0.00072	0.00105	0.00063
Vapour + NC viscosity	**Pa s**	NA	NA	NA	NA
Liquid sp. heat	**kJ kg^{-1} K^{-1}**	4.182	4.180	4.182	4.180
Vapour + NC sp. heat	**kJ kg^{-1} K^{-1}**	NA	NA	NA	NA
Liquid thermal conductivity	**W m^{-1} K^{-1}**	0.6485	0.6251	0.6002	0.6340
Vap. + NC thermal conduct.	**W m^{-1} K^{-1}**	NA	NA	NA	NA
Latent heat	**kJ kg^{-1}**	2241	2277	2130	2142
Surface tension	**N m^{-1}**	0.06685	0.07036	0.07331	0.06914
Dew pt/bubble pt	**°C**	109.0	98.0	151.8	147.9
Freeze pt/pour pt	**°C**	-5	-5	0	0
Inlet pressure	**bar**	1.6		5	
Allowable press. drop	**bar**	0.6		0.5	
Fouling resistance	**m^2 K W^{-1}**	0.0003		0.0002	
Heat exchanged	**MW**	28.75			
Min./max. operating temp	**°C**	30	60	13	47
Max. operating pressure	**bar**	3		6	
Min. design pressure	**bar**	2		5	
Relief valve set pressure	**bar**	3		6	
Design pressure	**bar**	4		7	
Cyclic service		☒		☒	
Materials		Carbon Steel		Carbon Steel	
Corrosion allowance	**mm**	1.1		1.0	
Line size	**mm**	644	644	597	597
Heat treatment		☒		☒	
Hazards		Respiratory and skin irritation upon physical contact, in the event of leakage		Moderately pressurised	

Insulation		NA		NA	
Cleaning		Once every 3 months		Once every 3 months	
Over design multiplier		1.4		2.0	

Remarks				
Rev no				
Eng/date				
Checked/date				
Approved/date				

6 Nomenclature

DP	Degree of polymerisation (n)	(-)
E	Total enzyme concentration in saccharification reactor	(mm^3(g starch)$^{-1}$)
E_{AMG}	Glucoamylase concentration in saccharification reactor	(mm^3(g starch)$^{-1}$)
E_a	α-Amylase concentration in saccharification reactor	(mm^3(g starch)$^{-1}$)
G_n	Concentration of oligosaccharide with polymerisation degree of n	(g dm^{-3})
G_{Large}	Total concentration of sugars with DP > 7	(g dm^{-3})
k	Proportional constant	(h^{-1})
$[H^+]$	Hydrogen ion concentration	(mol dm^{-3})
k_e	Glucoamylase limitation parameter	(mm^3(g starch)$^{-1}$)
k_{en}	a-amylase limitation parameter	(mm^3(g starch)$^{-1}$)
k_{esm}	Parameter in pH expression	(g dm^{-3})
k_{es1}	Parameter in pH expression	(mol H^+ dm^{-3})
k_{es2}	Parameter in pH expression	(dm^{-3} (mol H^+)$^{-1}$)
K_g	Glucose inhibition parameter	(g glucose dm^{-3})
$K_{m,n}$	Michelis-Menten constant for n-mer oligosaccharide	(g dm^{-3})
$k_{max,n}$	Maximal velocity for digestion rate of n-mer oligosaccharide	(h^{-1})
k_n	Proportional parameter for glucose formation or n-mer oligosaccharide	(h^{-1})
k_{n1}	Parameter in pH expression	(mol H^+ dm^{-3})
k_{n2}	Parameter in pH expression	(dm^{-3} (mol H^+)$^{-1}$)
$k_{n,m}$	Parameter in pH expression	(h^{-1})
k_s	Substrate limitation parameter	(g total starch dm^{-3})
$k_{Large,n}$	k_n adjusted for α-amylase concentration	(h^{-1})
MW_n	Molecular weight of glucose or an n-mer oligosaccharide	(g mol^{-1})
m	Exponential parameter	(-)
n	Degree of polymerisation	(-)
S_o	Total starch concentration after liquefaction	(g dm^{-3})
v_{Gn}	Cleavage rate of an n-mer oligosaccharide due to action of glucoamylase	(g dm^{-3} h^{-1})
$v_{max,n}$	Maximum reaction rate for an n-mer oligosaccharide	(g dm^{-3} h^{-1})
V_1	Liquefaction reactor volume	(m^3)
V_2	Saccharification reactor volume	(m^3)
t	Timescale	(s)
T	Temperature	(^oC)
ρ	Density	(kg m^{-3})
μ	Viscosity	(Pa s)

7 References

[1] Akerberg C., Zacchi G., Torto N. & Gordon L., In: A kinetic model for enzymatic wheat starch saccharification, J Chemical Technology Biotechnology, 75, 306-314, 2000.

[2] Andres Illanes, Enzyme Biocatalysis Principles and Applications, Springer, 2008, chapter 5 p. 205-230.

[3] J. R. Couper, W. R. Penney, Chemical Process Equipment Selection and Design, Elsevier, 2005, 2nd edition, chapter 11 p.329-337, chapter 18 p.654-656, chapter 19 p.665-671.

[4] Perry, Robert H, and Don W. Green, Perry's Chemical Engineers' Handbook, New York: McGraw-Hill, 2008, 7th edition, chapter 2 p.183-188, chapter 7 p.3-14, chapter 23 p.3-27.

[5] L. F.Albright, Albright's Chemical Engineering hand-book, CRC Press Taylor and Francis group, chapter 9 p.623-629 & 644-652 & 697-705.

[6] P. M. Doran, Bioprocess Engineering Principles, Academic Press 2012, 2nd edition, chapter 8 p.255-298, chapter 14 p.773-778 & 820-823.

[7] S. H. Loeventhal, In: Design of power transmitting shafts, https://ntrs.nasa.gov/search.jsp (accessed on May 10 2020).

[8] ASM Aerospace Specification Metals Inc., In: 'AISI Type 304 stainless steel' ferrous metal, Heat Resisting; Metal; Stainless Steel; T 300 Series Stainless Steel, 800 398-4345, http://asm.matweb.com (accessed on May 12 2020).

[9] S. Chatterjee, In: Production and estimation of alkaline protease by immobilised *Bacillus licheniformis* isolated from poultry farm soil of 24 Parganas and its reusability, Journal of Advanced Pharmaceutical Technology and Research, Vol. 6, p. 2-6, 2015.

[10] T. Komaki et al., In: Studies on Enzymatic Liquefaction and Saccharification of Starch, Agr. Biol. Chem, Vol. 32, No. 3, pp. 314-319, 1968.

[11] A. Plonka, Dispersive kinetics, Springer, 2001, p.43-47

8 Appendices

8.1 Tables of parameters used from the kinetic data presented by Akerberg et al.

Table 13: List of certain kinetic parameter values employed in the design

Substrate	n	$K_{m,n}$ / g dm^{-3}	$k_{max,n}$ / 10^4 h^{-1}
Maltose	2	0.157	1.74
Maltotriose	2	0.203	3.59
Maltotetraose	3	0.182	6.01
Maltopentaose	4	0.167	7.60
Maltohexaose	5	0.0990	5.76
Maltoheptaose	6	0.139	7.31

Table 14: Temperature dependence of certain kinetic parameters employed in the design

Parameter	Temperature	
	30 C°	55 C°
k_{esm} / 10^{13} g dm^{-3}	5.29	266
$k_{1,m}$ / h^{-1}	0.801	0.720
$k_{2,m}$ / h^{-1}	0.782	0.155
$k_{3,m}$ / h^{-1}	0.275	0.359
$k_{4,m}$ / h^{-1}	0.344	0.390
$k_{5,m}$ / h^{-1}	0.398	0.403
$k_{6,m}$ / h^{-1}	0.0921	0.347
$k_{7,m}$ / h^{-1}	0.528	0.869

Table 15: Additional kinetic parameters employed in the design. Parameters k_{n1} and k_{n2} were assumed to remain constant for n=1-7

K_g / g glucose dm^{-3}	110
k_e / 10^{11} mm^3 amyloglucosidase (g total starch)$^{-1}$	1.06
k_s / 10^8 (g total starch) dm^{-3}	1.77
k_{en} / mm^3 α-amylase (g total starch)$^{-1}$	0.309
k_{es1} / 10^{-6} mol H^+ dm^{-3}	3.32
k_{es2} / 10^4 dm^3 (mol H^+)$^{-1}$	2.64
k_{n1} / 10^{-7} dm^3 (mol H^+)$^{-1}$	1.97
k_{n2} / 10^3 dm^3 (mol H^+)$^{-1}$	3.61

8.2 Ordinary differential equations used to model the saccharification process and their dependence on pH, E_a, E_{AMG}, and S_o (Akerberg et al. 2000).

In the model used to describe the saccharification process, the long oligosaccharide chains with DP > 7 were treated as one species. The rest with 1 < n < 7 were treated as individual species. Equations 1-4 describe the rate of change of sugar polymers spanning from G_1 to G_7 including G_{large}.

$$\frac{dG_{Large}}{dt} = -(\sum_{n=1}^{7} k_{Large,n})G_{large} \quad (1)$$

$$\frac{dG_7}{dt} = v_{Gn} + k_{Large,7} G_{Large} \tag{2}$$

$$\frac{dG_n}{dt} = v_{Gn} - v_{Gn+1} \frac{MW_n}{MW_{n+1}} + k_{large,n} G_{Large} \qquad \text{for } 2 \leq n \leq 6 \tag{3}$$

$$\frac{dG_1}{dt} = -\left(\sum_{j=3}^{7} v_{G_j} \frac{MW_1}{MW_j}\right) - 2v_{G_2} \frac{MW_1}{MW_2} + k_{large,1} G_{Large} \tag{4}$$

In equation 3, MW_n refers to the molecular weight of a sugar with degree of polymerisation n. This can be found via the relationship depicted in equation 5.

$$MW_n = 180n - 18(n-1) \tag{5}$$

The rate constant $k_{Large,n}$ is dependent on pH and α-amylase concentration E_a. Equation 6 depicts this. Furthermore, equation 6 shows the dependence of cleavage rate $V_{G,n}$ on pH and glucoamylase concentration E_{AMG}.

$$k_{Large,n} = \left(\frac{k_{n,m}}{1 + \frac{k_{n1}}{[H^+]} + k_{n2}[H^+]}\right)\left(\frac{E_a}{E_a + k_{en}}\right) \tag{6}$$

$$v_{G,n} = -\left(\frac{v_{max,n} G_n}{K_{m,n}}\right)\left(\frac{K_g}{K_g + G_1}\right) \tag{7}$$

$$v_{max,n} = \left(\frac{k_{esm}}{1 + \frac{k_{es1}}{[H^+]} + k_{es2}[H^+]}\right)\left(\frac{k_{max,n} E_{AMG}}{E_{AMG} + k_e}\right)\left(\frac{S_0}{S_0 + k_s}\right) \tag{8}$$